Tumor-Secreted Lysophostatidic Acid Accelerates Hepatocellular Carcinoma Progression by Promoting Differentiation of Peritumoral Fibroblasts in Myofibroblasts

Antonio Mazzocca,[1] Francesco Dituri,[1] Luigi Lupo,[2] Michele Quaranta,[3]
Salvatore Antonaci,[1] and Gianluigi Giannelli[1]

Hepatocellular carcinoma (HCC) occurs in fibrotic liver as a consequence of underlying cirrhosis. The goal of this study was to investigate how the interaction between HCC cells and stromal fibroblasts affects tumor progression. We isolated and characterized carcinoma-associated fibroblasts (CAFs) and paired peritumoral tissue fibroblasts (PTFs) from 10 different patients with HCC and performed coculture experiments. We demonstrated a paracrine mechanism whereby HCC cells secrete lysophostatidic acid (LPA), which promotes transdifferentiation of PTFs to a CAF-like myofibroblastic phenotype. This effect is mediated by up-regulation of specific genes related to a myo/contractile phenotype. After transdifferentiation, PTFs expressed α-smooth muscle actin (α-SMA) and enhanced proliferation, migration, and invasion of HCC cells occur. A pan-LPA inhibitor (α-bromomethylene phosphonate [BrP]-LPA), or autotaxin gene silencing, inhibited this PTF transdifferentiation and the consequent enhanced proliferation, migration, and invasion of HCC cells. *In vivo*, PTFs coinjected with HCC cells underwent transdifferentiation and promoted tumor progression. Treatment with BrP-LPA blocked transdifferentiation of PTFs, downregulated myofibroblast-related genes, and slowed HCC growth and progression. Patients with larger and metastatic HCC and shorter survival displayed higher serum levels of LPA. Analysis of microdissected tissues indicated that stroma is the main target of the LPA paracrine loop in HCC. As a consequence, α-SMA–positive cells were more widespread in tumoral compared with paired peritumoral stroma. *Conclusion:* Our data indicate that LPA accelerates HCC progression by recruiting PTFs and promoting their transdifferentiation into myofibroblasts. Inhibition of LPA could prove effective in blocking transdifferentiation of myofibroblasts and tumor progression. (HEPATOLOGY 2011;54:920-930)

In Western countries, hepatocellular carcinoma (HCC) develops in patients with liver cirrhosis and is the final stage of a disease that can last for many years.[1,2] It is generally accepted that HCC originates from hepatocytes but grows and advances while fully embedded in a surrounding microenvironment

with a rich content of myofibroblasts, fibroblasts, and other cell types due to the underlying cirrhosis. Liver myofibroblasts, derived from quiescent fibroblasts and hepatic stellate cells activated by the chronic injury, can be recognized by their expression of α-smooth muscle actin (α-SMA).[3,4] Myofibroblasts have been detected at the advancing edge of several different malignancies as the predominant phenotype in the cancer-associated fibroblast (CAF) population.[5]

Although the origin of CAFs is still controversial, their immunophenotypical characterization, which primarily includes α-SMA and excludes epithelial and endothelial common markers, is widely accepted.[3,6,7] CAFs differ from peritumoral tissue fibroblasts (PTFs) not in terms of somatic mutations but rather molecular and functional differences in modulating neighboring cancer cells.[8,9] However, the paracrine cross-talk between HCC and stromal fibroblasts such as CAFs or PTFs is still poorly understood.

HCC is recognized as a highly heterogeneous tumor because of its complex multistep pathogenesis, which is further complicated by the preexisting liver cirrhosis. For this reason, the identification of a proper biological target is essential in order to design suitable molecular-oriented therapy.

Lysophosphatidic acid (LPA) is a potent bioactive lipid, produced by hydrolysis of lysophosphatidylcholine by autotaxin (ATX). ATX, which is also known as ectonucleotide pyrophosphatase/phosphodiesterase family member 2, is an enzyme that was first identified as an autocrine motility factor because it is capable of promoting migration of melanoma cells.[10] ATX is an important mediator of tumor progression and plays a key role in cancer progression either as a motile factor or by producing LPA. LPA is a bioactive lipid implicated in several functions, including proliferation, apoptosis, migration, and cancer cell invasion.[11] It was shown recently that the ATX/LPA pathway that activates LPA receptor 1 (LPA1) promoted cell invasion in an *in vitro* experimental model of HCC.[12]

In this study, we demonstrate that secretion of LPA by HCC cells promotes transdifferentiation of stromal peritumoral fibroblasts to myofibroblasts, and that this accelerates tumor progression. Consistently, LPA is shown to be increased in patients with more advanced disease and, finally, myofibroblasts are more expressed in HCC compared with paired peritumoral tissue.

Materials and Methods

Samples of HCC and paired adjacent liver tissue were obtained from 10 patients (Supporting Table 2) undergoing liver resection. Approval for the study was obtained from the local ethics committee, and patients gave prior written informed consent for the use of their tissues. Peritumoral and HCC tissues were minced with scalpels in a tissue culture dish and then enzymatically dissociated in Dulbecco's modified Eagle's medium/F12 medium supplemented with 0.1 % bovine serum albumin, 100,000 U/L penicillin G, 100 mg/L streptomycin, 1.0 g/mL fungizone, 500 units/mL collagenase D (Invitrogen), and 100 U/mL hyaluronidase (Calbiochem) at 37°C for 16 hours. The suspension was then centrifuged at 500 rpm (80g) for 5 minutes to separate the epithelial and fibroblast cells. Fibroblasts in the supernatant were pelleted by way of centrifugation at 800 rpm (100g) for 10 minutes, followed by two washes with Dulbecco's modified Eagle's medium/F12 medium. Fibroblast antigen-positive cells were isolated from the cell pellet through positive selection using anti-fibroblast MicroBeads and the MS Column (Miltenyi Biotec) according to the manufacturer's instructions. Isolated cells were resuspended in Iscove's modified Dulbecco's medium supplemented with 20% fetal bovine serum (Invitrogen) and 5 μg/mL insulin and plated in 25 cm^2 tissue culture flasks. The cultures were then incubated at 37°C at 5% CO$_2$. Primary cultures of PTFs and CAFs isolated from human HCC tumors were immunophenotypically characterized by way of positive immunostaining for fibroblast markers and distinguished from tumor cells by negative staining for pan-cytokeratin, Hepar-1, E-cadherin, and α-fetoprotein (Supporting Fig. 1). Purity of the isolated fibroblast population, assessed by way of immunostaining, was >99%. Cells from passages 3-10 were used for all experiments.

Full descriptions of additional Materials and Methods are given in the Supporting Information.

Results

First, we stained HCC and matching peritumoral tissues with an anti–α-SMA antibody to detect stromal myofibroblasts.[3] We found that α-SMA–positive cells were mostly present in the fibrotic septa of the peritumoral cirrhotic tissue, whereas in tumor tissues α-SMA–positive cells were mainly expressed within the tumor stroma (Fig. 1A). We then isolated and further characterized CAFs and PTFs from 10 different patients using a panel of epithelial and mesenchymal antigens (Fig. 1B,C and Supporting Fig. 1A).

Consistent with the microscopic observation, the number of vimentin-positive cells was similar in PTFs and CAFs preparations, whereas the number of α-SMA–positive cells was much higher ($P < 0.0001$) in CAFs
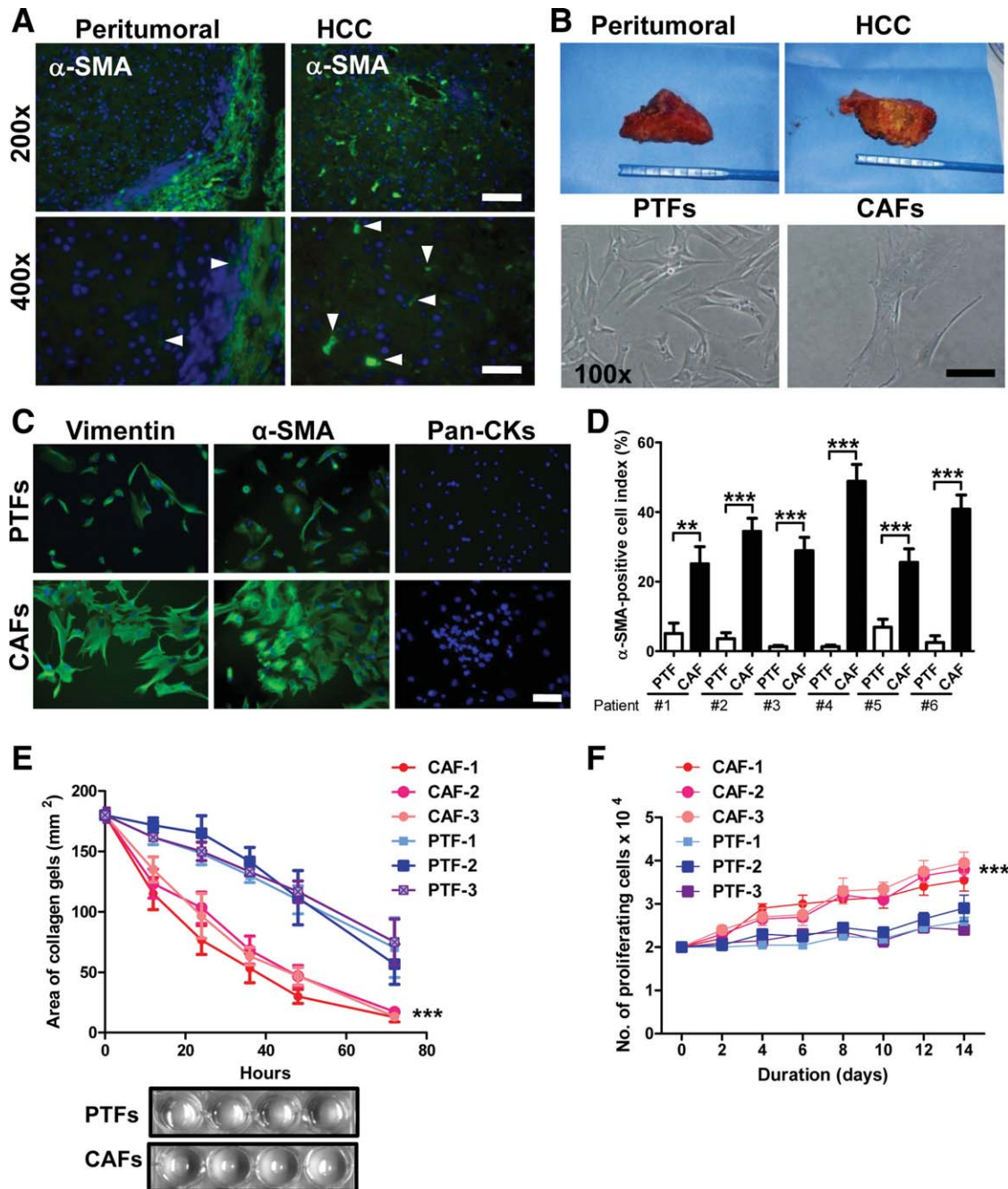
Fig. 1. Phenotypic and functional characterization of PTFs and CAFs isolated from patients with HCC. (A) Representative immunofluorescence images showing the distribution of α-SMA–positive cells in peritumoral and HCC tissues. Scale bar, 50 μm. (B) Representative images showing surgical specimens of human HCC from which PTFs and CAFs were isolated (top panels) and phase-contrast micrographs of PTFs and CAFs displaying their morphology in culture (bottom panels). Scale bar, 50 μm. (C) Immunophenotypical characterization of PTFs and CAFs from HCC patients. Fibroblasts were immunostained with anti-vimentin, anti–α-SMA (markers for mesenchymal cells), and anti–pan-cytokeratin (a marker for endothelium) antibodies. Scale bar, 50 μm. (D) Quantification of α-SMA–positive cells in PTF and CAF populations. Cells were evaluated as fractions of the total cell number and were counted in six independent fields under a fluorescence microscope. **$P < 0.01$. ***$P < 0.001$. (E) Collagen gel contraction assay of PTFs and CAFs isolated from three different patients with HCC. The contracted gel areas were measured at different time points (between 12 and 72 hours). A representative image showing the appearance of the contracted gels of PTFs and CAFs at 72 hours (bottom panels). Error bars show the SEM. ***$P < 0.001$ (two-way analysis of variance [ANOVA]). (F) Kinetics of proliferation of PTFs and CAFs isolated from three different patients with HCC. Assays were run in triplicate, and error bars show the SEM of three independent experiments. ***$P < 0.001$ (two-way ANOVA).

compared with PTFs (Fig. 1D and Supporting Fig. 1B). No staining was observed in either cell population for pan-cytokeratin, nor for other epithelial or vascular markers (Fig. 1C), thus indicating the absence of contamination by other cell types. These results were reproducible in all the different preparations (six out of 10 are shown).
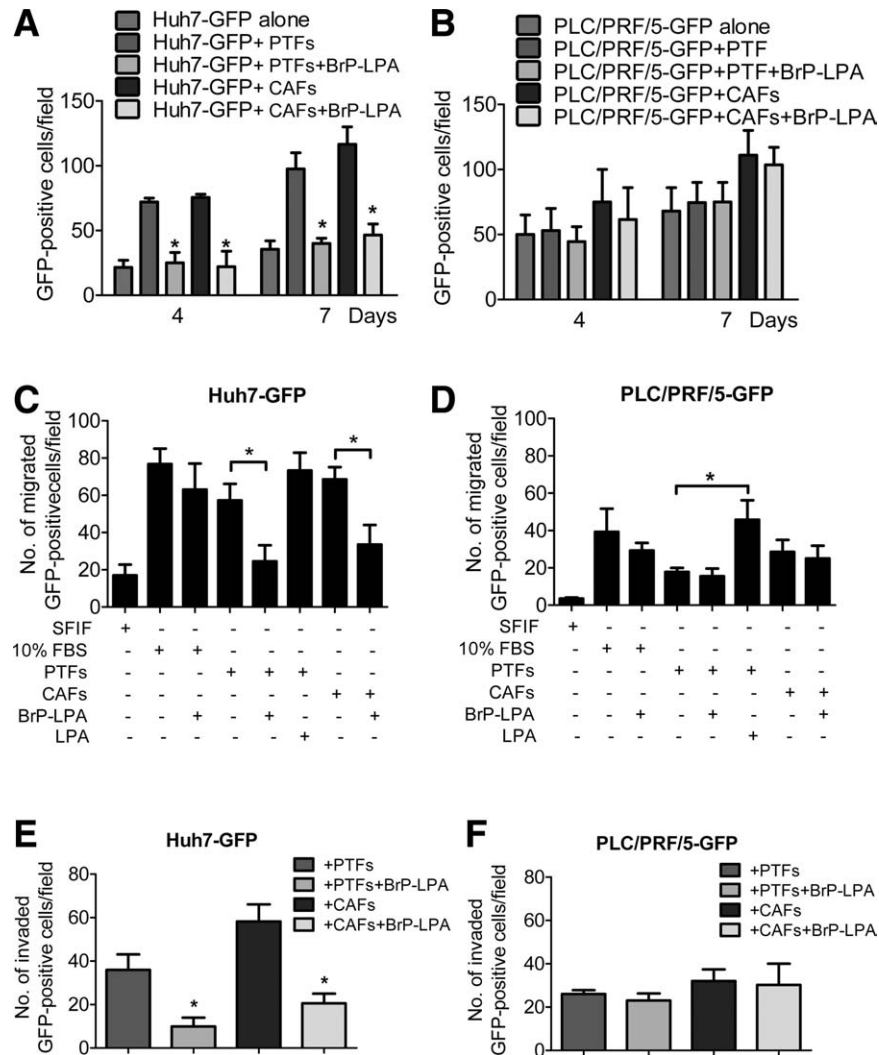
Fig. 2. HCC growth, migration, and invasion are enhanced by PTFs and CAFs stimulated by the paracrine action of LPA secreted by tumor cells. (A) Cell growth of Huh7-green fluorescent protein (Huh7-GFP) in coculture with PTFs and CAFs and in the presence of 10 μM of BrP-LPA or control evaluated in three-dimensional (3D) gel collagen assays on days 3 and 7. *$P < 0.05$. (B) Cell growth of PLC/PRF/5-GFP in cocultures with PTFs and CAFs and in the presence of 10 μM of BrP-LPA or control evaluated in 3D gel collagen assays on days 3 and 7. The morphology and density of PLC/PRF/5-GFP in 3D cocultures on collagen gels is also shown (bottom panel). (C) Effect of BrP-LPA on Huh7-GFP migration in the presence or absence of PTFs and CAFs. Assays were performed at 72 hours, and GFP-positive cells were counted in at least six random fields. *$P < 0.05$. (D) Effect of BrP-LPA on PLC/PRF/5-GFP migration in the presence or absence of PTFs and CAFs. Assays were performed at 72 hours, and GFP-positive cells were counted in at least six random fields. (E) Effect of BrP-LPA on Matrigel invasion of Huh7-GFP in the presence or absence of PTFs and CAFs. Assays were performed at 72 hours, and GFP-positive cells were counted in at least six random fields. *$P < 0.05$. (F) Effect of BrP-LPA on Matrigel invasion of PLC/PRF/5-GFP in the presence or absence of PTFs and CAFs. Assays were performed at 72 hours, and GFP-positive cells were counted in at least six random fields. Error bars show the SEM of three independent experiments, each conducted in triplicate.

The different expression of α-SMA between CAFs and PTFs also reveals different functions. CAFs display a greater ability to contract collagen gel ($P < 0.0001$) and to proliferate more efficiently over time up to 14 days ($P < 0.001$) compared with PTFs (Fig. 1 E,F and Supporting Fig. 1C,D). These results were consistently reproduced in all the different cell preparations.

In coculture experiments, both CAFs and PTFs stimulated Huh7 proliferation with the same efficiency in a three-dimensional collagel gel after 4 ($P < 0.05$)

and 7 ($P < 0.05$) days (Supporting Fig. 2). However, in the same experiments, the addition of α-bromomethylene phosphonate [BrP]-LPA, a pan-LPA inhibitor, blocked the proliferation rate of Huh7 cells ($P < 0.05$) stimulated by the presence of PTFs or CAFs (Fig. 2A). Notably, under the same experimental conditions, there was only a trend toward an increased proliferation of PLC/PRF/5 cells upon CAFs treatment, whereas BrP-LPA abolished the CAFs-dependent PLC/PRF/5 proliferation (Fig. 2B). In cell motility

experiments, Huh7 cells migrated more efficiently in the presence of PTFs compared with control ($P <$ 0.05), and even more efficiently in the presence of CAFs. However, the presence of BrP-LPA significantly inhibited tumor migration ($P < 0.05$) (Fig. 2C). PLC/PRF/5 cells showed a similar trend, although the efficiency of migration was much lower than that of Huh7 cells (Fig. 2D). In addition, invasion of Huh7 cells through Matrigel was increased in the presence of PTFs and was blocked when BrP-LPA was added. The invasive capability of Huh7 cells was enhanced in the presence of both PTFs and CAFs and was inhibited in the presence of BrP-LPA (Fig. 2E). Conversely, PLC/PRF/5 showed a poor invasive capacity through Matrigel in the presence of either PTFs or CAFs. Therefore, BrP-LPA did not display any effect on these cells (Fig. 2F). No toxicity effect was observed at used concentration on Huh7 cells, PLC/PRF/5 cells, PTFs, or CAFs as evaluated by MTT assay (Supporting Fig. 3). In conclusion, PTFs and CAFs increased the aggressive phenotype in Huh7 cells but not in PLC/PRF/5 cells.

To gain a better insight into the molecular mechanisms underlying the paracrine cross-talk between stromal and HCC cells, we studied the paracrine action of LPA. We first measured the concentrations of secreted LPA in conditioned medium from PTFs and CAFs and in two different HCC cell lines (Huh7 and PLC/PRF/5). High levels of LPA were detected in Huh7 cells compared with PLC/PRF/5 cells, CAFs, and PTFs ($P < 0.0001$) (Fig. 3A). We then analyzed the messenger RNA (mRNA) expression levels of LPA receptors 1-5 in the same cells. We found that among the LPA receptors investigated, LPA receptor 1 was the most strongly expressed, being mainly expressed by CAFs and PTFs compared with Huh7 cells (Fig. 3B). In agreement with the LPA levels, ATX expression levels were more abundant in Huh7 compared with PLC/PRF/5 cells, CAFs, and PTFs ($P < 0.0001$) (Supporting Fig. 4A). In conclusion, Huh7 cells produced LPA and ATX, whereas PLC/PRF/5cells, PTFs, and CAFs did not, and CAFs and PTFs only expressed LPA receptors.

To investigate the functional role of PTFs or CAFs in the cross-talk between stromal and HCC cells, we challenged PTFs to migrate in the presence of Huh7- and PLC/PRF/5-conditioned medium (CM). In the presence of Huh7-CM, PTFs migrated efficiently to the same extent as in the presence of LPA. This effect was already evident after 12 hours but was stronger after 72 hours. BrP-LPA blocked this migration (Fig. 3C). On the contrary, no PTF migration was observed in the presence of PLC/PRF/5-CM. Therefore, BrP-

LPA did not display any effect on this coculture, whereas the addition of LPA still promoted strong migration (Fig. 3D).

Moreover, the number of α-SMA–positive cells was increased in PTFs migrating in the presence of Huh7-CM and LPA, but was strongly reduced by BrP-LPA ($P < 0.05$). This effect was particularly evident after 72 hours (Fig. 3E). On the contrary, the number of α-SMA–positive cells was not increased in PTFs migrating in the presence of PLC/PRF/5-CM, but was strongly increased when exogenous LPA was added (Fig. 3F). Similar results were obtained with Hep3B and HLE, LPA-producing and nonproducing, respectively, as shown in Supporting Fig. 5. In conclusion, Huh7 cells recruited and activated PTFs through the secretion of LPA, but PLC/PRF/5-CM did not.

To confirm the role of LPA as a paracrine mediator of stromal–tumor interaction, we knocked down the ATX gene, a major LPA-producing enzyme, in Huh7 cells and performed coculture experiments. ATX-silenced cells secreted low levels of LPA compared with control ($P < 0.0001$), as evaluated by enzyme-linked immunosorbent assay (ELISA) measurement of LPA in Huh7-CM (Supporting Fig. 4B). More importantly, low levels of LPA in ATX-silenced Huh7 determined a significant reduction of tumor proliferation and migration in cocultures with CAFs and PTFs compared with control ($P < 0.05$). The addition of exogenous LPA to ATX-silenced cells partially restored their capability to proliferate and migrate (Supporting Fig. 4C,D).

To further study the effect of LPA in this context, we stimulated PTFs and CAFs with LPA. As shown above, the number of α-SMA–positive cells was higher in the CAF population than in the PTF population. However, treatment with LPA strongly increased the number of α-SMA–positive cells in the PTF population but not in the CAF population ($P < 0.005$). Moreover, treatment with BrP-LPA blocked this effect (Fig. 4A,B). Consistently, LPA increased the ability of PTFs to contract collagen gel compared with control ($P < 0.001$). This effect was mild on CAFs ($P < 0.05$), a phenotype with an intrinsic ability to contract collagen gel (Fig. 4C). Furthermore, LPA significantly stimulated proliferation of PTFs over time, but not of CAFs ($P < 0.001$) (Fig. 4D). To explain the phenotypic changes in PTFs induced by LPA, we investigated the behavior of several genes under LPA stimulation. Among the investigated genes, we identified a gene signature responsible for the transdifferentiation of PTFs to a CAF-like myofibroblastic phenotype (Fig. 4E,F).

To test the reliability *in vivo* of the mechanism described *in vitro*, we assayed the tumorigenicity of
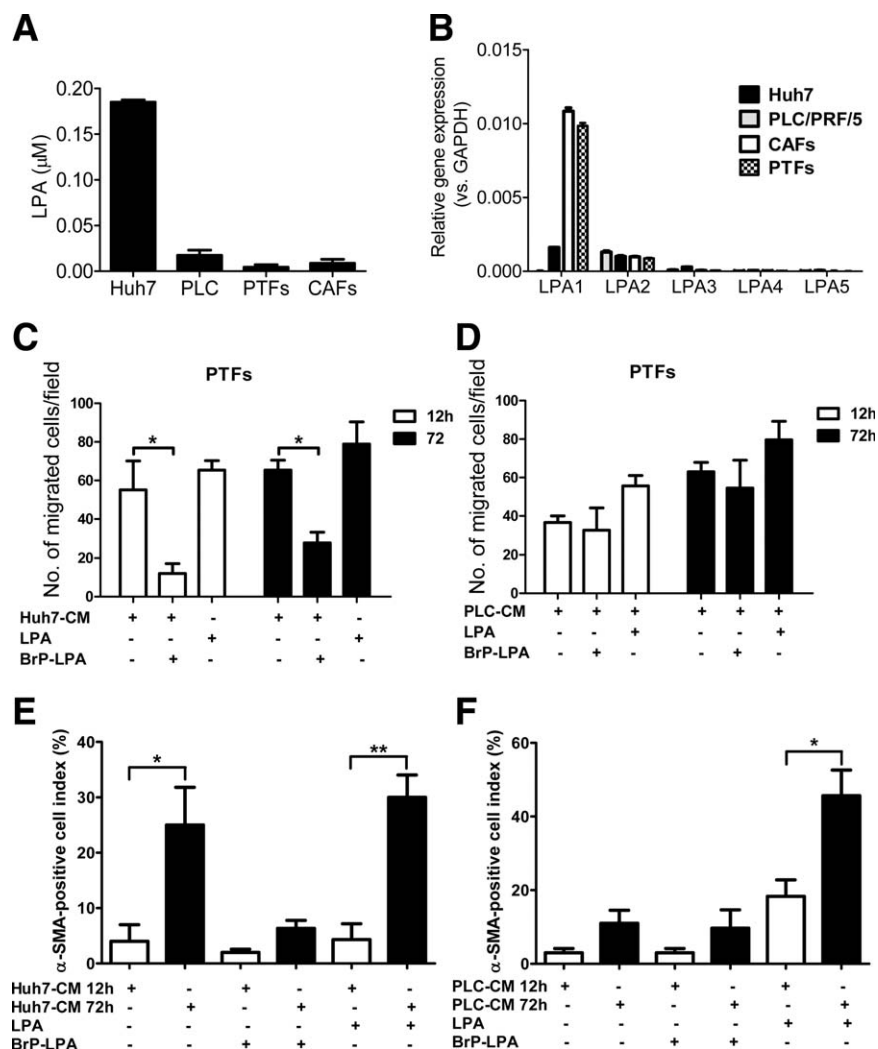
Fig. 3. HCC cells recruit PTFs and promote their differentiation to a CAF-like myofibroblastic phenotype by secreting LPA. (A) LPA level in conditioned medium from PTFs and CAFs and two different HCC cell lines (Huh7 and PLC/PRF/5) measured with the LPA ELISA colorimetric assay. (B) mRNA expression levels of LPA receptors in PTFs, CAFs, and two different HCC cell lines (Huh7 and PLC/PRF/5) evaluated by way of real-time PCR. Results are expressed as the ratio of the number of LPA receptors/glyceraldehyde 3-phosphate dehydrogenase (GAPDH) copies and represent the mean $\pm$ SEM of three separate experiments, each conducted in triplicate. (C) Effect of soluble factors (conditioned medium) from Huh7 and LPA (10 μM) on PTF migration/recruitment in the presence or absence of BrP-LPA (10 μM). Assays were performed at 12 or 72 hours, and cells were counted in at least six random fields. *$P < 0.05$. (D) Effect of soluble factors (conditioned medium) from PLC/PRF/5 alone or with LPA on PTF migration/recruitment in the presence or absence of BrP-LPA (10 μM). Assays were performed at 12 or 72 hours, and cells were then counted in at least six random fields. (E) Quantification of α-SMA–positive cells in migrated PTFs in the presence of Huh7-CM and LPA (10 μM) with or without BrP-LPA (10 μM). At 12 or 72 hours, filters were fixed and migrated cells were stained for α-SMA and DAPI. α-SMA–positive cells were evaluated as a fraction of the total cell number and counted in six independent fields under a fluorescence microscope. *$P < 0.05$. **$P < 0.01$. (F) Quantification of α-SMA–positive cells in PTFs migrated toward PLC/PRF/5-CM alone or with LPA (10 μM) in the presence or absence of BrP-LPA (10 μM). At 12 or 72 hours, filters were fixed and migrated cells were stained for α-SMA and 4',6-diamidino-2-phenylindole. α-SMA–positive cells were evaluated as a fraction of the total cell number and counted in six independent fields under a fluorescence microscope. *$P < 0.05$. Error bars show the SEM of three independent experiments, each conducted in triplicate.

Huh7 cells in a xenograft model of HCC. Huh7, injected alone, formed tumors within 3 weeks after injection, with a further increase of the tumor mass in the next 3 weeks. However, when coinjected with CAFs, Huh7 cells formed larger tumors faster ($P < 0.01$), after only 2 weeks. Furthermore, Huh7 cells coinjected with PTFs provoked a greater development of tumors ($P < 0.05$), whereas treatment with BrP-

LPA dramatically reduced tumor growth after the first three drug administrations ($P < 0.01$) (Fig. 5A). In tumors originated by coinjection of Huh7 cells with PTFs, we detected a large number of α-SMA–positive cells (control group). Conversely, in tumors originated from the same cells but treated with BrP-LPA, the number of α-SMA–positive cells was significantly decreased (treated group) (Fig. 5B). Next, we evaluated
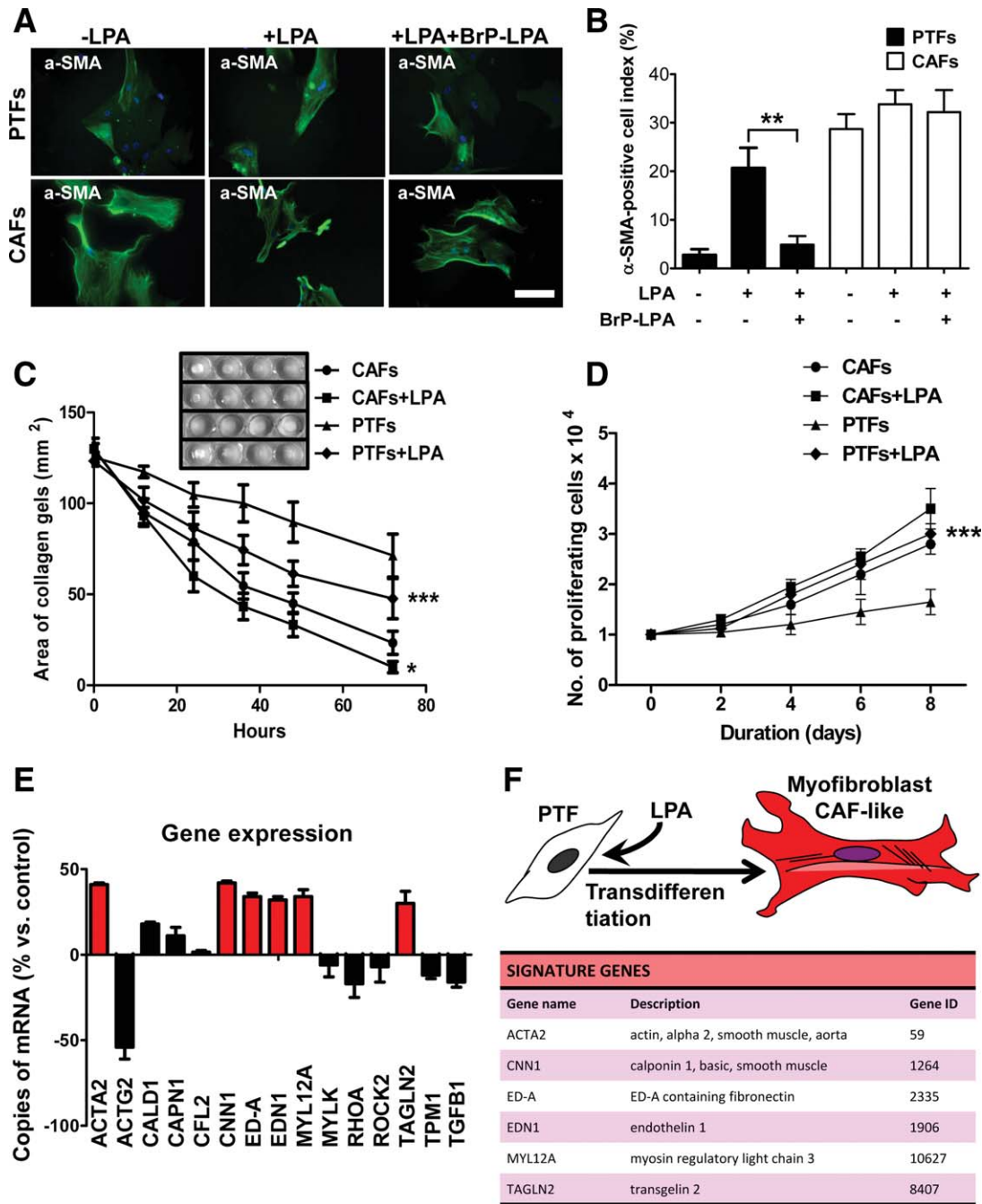
Fig. 4. LPA-driven PTF differentiation to a CAF-like myofibroblastic phenotype is supported by activation of specific genes. (A) Representative immunofluorescence images of PTFs and CAFs showing α-SMA–positive staining upon stimulation of LPA (10 μM) and in the presence of 10 μM BrP-LPA. Scale bar, 50 μm. (B) Quantification of α-SMA–positive cells in PTF and CAF populations upon stimulation with 10 μM of LPA and in the presence of 10 μM BrP-LPA. Cells were evaluated as a fraction of the total cell number and counted in six independent fields under a fluorescence microscope. **$P < 0.01$. (C) Collagen gel contraction assay of PTFs and CAFs in the presence of 10 μM LPA or control. The contracted gel areas were measured at different time points (between 12 and 72 hours). Representative image shows the appearance of the contracted gels of PTFs and CAFs at 72 hours. *$P < 0.05$. ***$P < 0.001$ (two-way ANOVA). (D) Kinetics of proliferation of PTFs and CAFs in the presence of 10 μM LPA or control. Assays were performed in triplicate, and error bars show the SEM of three independent experiments.***$P < 0.001$ (two-way ANOVA). (E) Expression of a myofibroblastic phenotype gene signature by PTFs undergoing transdiffentiation to a myofibroblast upon stimulation with LPA evaluated by way of real-time PCR. Results are expressed as the mean $\pm$ SEM of three separate experiments, each conducted in triplicate. (F) Model showing transdiffentiation to a myofibroblast phenotype of LPA-treated-PTFs. A list of the genes included in the gene signature is shown.

whether the gene signature identified in cultured PTFs stimulated with LPA was affected in mice following treatment with BrP-LPA. We found that genes that

were up-regulated *in vitro* were inhibited in BrP-LPA-treated tumors (Fig. 5C). To ensure the specificity of our model, we investigated the expression of human
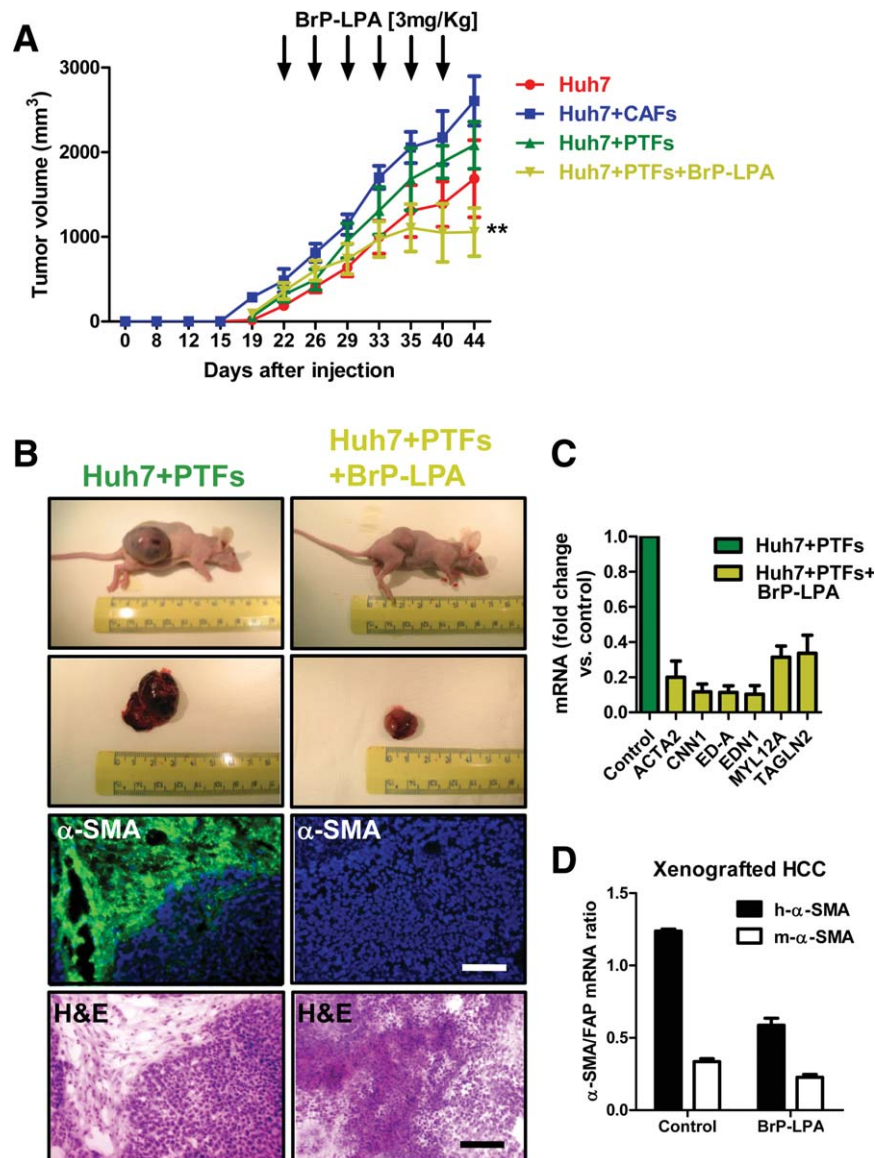
Fig. 5. Inhibition of LPA arrests tumor progression by blocking PTF differentiation to a CAF-like myofibroblastic phenotype in a xenograft model of HCC. (A) Effect of PTFs and CAFs on HCC growth when coinjected intradermally with Huh7 cells. The schedule of treatments with BrP-LPA (3 mg/kg intraperitoneally) is marked with arrows. Tumors resulting from coinjection with CAFs and Huh7 cells were larger and developed earlier than in controls (Huh7 cells injected alone). Tumors resulting from coinjection with PTFs and Huh7 displayed an intermediate phenotype. However, tumors resulting from coinjection with PTFs and Huh7 cells, treated with BrP-LPA to inhibit the transdifferentiation to a CAF-like myofibroblastic phenotype, were significantly smaller than controls (saline). **$P < 0.01$ (two-way ANOVA). (B) Reduced tumor volumes in the flank of nude mice coinjected with PTFs and Huh7 cells following treatment with 3 mg/kg BrP-LPA (right panels) compared with controls (left panels). Each data point is the mean ± SEM of at least 10 tumors. Scale bar, 50 μm. (C) Change in the myofibroblastic phenotype gene signature expression following treatment with BrP-LPA in mice. Total RNA was extracted from tumor tissues and gene expression was evaluated by way of real-time PCR and expressed as mRNA-fold change versus control. (D) Quantification of mouse (m) and human (h) α-SMA expression in xenografted HCC tumors resulting from coinjection with PTFs and Huh7 cells treated with BrP-LPA or control to inhibit the transdifferentiation to a CAF-like myofibroblastic phenotype. α-SMA gene expression was measured by way of real-time PCR and expressed as a ratio of the unvaried gene expression of the fibroblast activation protein (FAP). Error bars show the SEM of three independent experiments.

and mouse α-SMA in xenografted HCC originated by coinjection of Huh7 with PTFs and by the same coinjection then treated with BrP-LPA. h-α-SMA was more strongly expressed than mouse α-SMA, as measured by real-time polymerase chain reaction (PCR), and in drug-treated animals the human isoform of

α-SMA but not the murine isoform was down-regulated, suggesting that injected PTFs were still present and functionally active at the end of the experiment, and also that the presence of host/resident myofibroblasts did not significantly affect results (Fig. 6D). In conclusion, we demonstrated that LPA secreted by
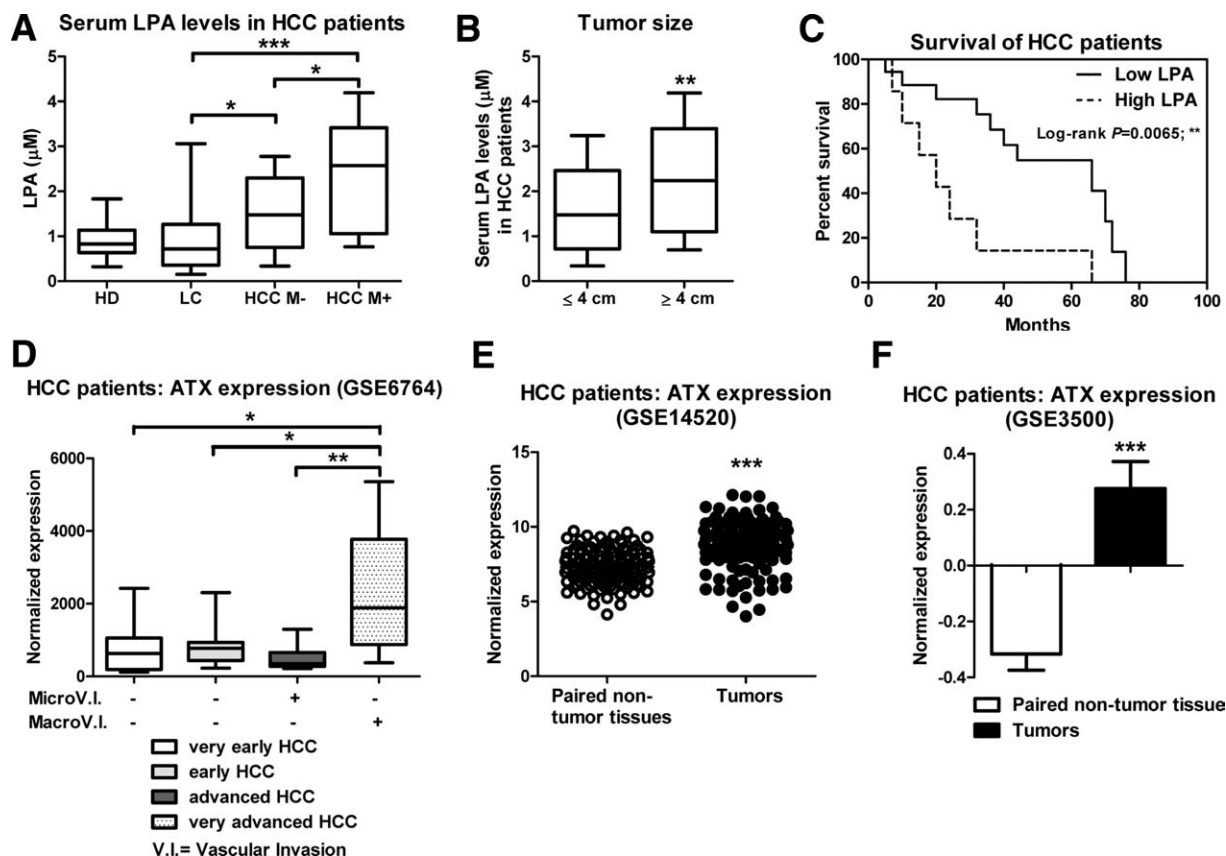
Fig. 6. Clinical evidence of the role of LPA in patients with HCC. (A) LPA levels in human serum samples from healthy donors (HD), patients with liver cirrhosis (LC), and patients with HCC with (HCC M+) and without metastasis (HCC M−) measured by way of LPA ELISA colorimetric assay. Data are shown as box and whisker plots, and P values were calculated by way of two-tailed Student t test.*$P < 0.05$. ***$P < 0.001$ (B) Box and whisker plot showing the correlation between LPA serum levels and tumor size. Serum LPA levels are increased in HCC patients with larger tumors compared with those with smaller tumors. P values were calculated by way of two-tailed Student t test. **$P < 0.01$. (C) LPA expression levels are correlated with survival in HCC patients. In log-rank analyses, low serum LPA levels (≤ 2 μM) predict a longer survival of HCC patients than high serum levels (>2 μM). **$P = 0.0065$ (log-rank test). (D) Expression levels of ATX, a major LPA-producing enzyme, are increased during HCC progression. Data from the Wurmbach cohort (GSE6764)[13] showing that ATX expression levels are increased in HCC tissues of patients with macrovascular invasion (n = 10) compared with microvascular invasion (n = 7; **$P = 0.0096$) and to HCC patients with very early (n = 7; *$P = 0.0492$) or early disease (n = 10; *$P = 0.0208$). (E,F) Data from (E) the Wang cohort (GSE14520) showing increased expression levels of ATX in HCC tissues (n = 129) compared with peritumoral tissues (n = 126; ***$P < 0.0001$) and (F) the Chen cohort (GSE3500; http://www.ncbi.nlm.nih.gov/geo/query/acc.cgi?acc=GSE3500) showing increased expression levels of ATX in HCC tissues (n = 79) compared with peritumoral tissues (n = 69; ***$P < 0.0001$). Error bars show the SEM.

HCC cells recruits and activates PTFs, orchestrating their differentiation to a CAF-like myofibroblastic phenotype which, in turn, accelerates HCC progression.

Finally, we aimed to validate these findings in HCC patients. We therefore analyzed LPA serum levels in 60 patients with HCC (30 patients with and 30 without metastases), and in 50 patients with liver cirrhosis. We found that LPA serum levels were higher in HCC compared with liver cirrhosis patients ($P < 0.05$). Among HCC patients, LPA serum levels were significantly ($P < 0.05$) higher in those with metastasis compared with those without (Fig. 6A). Patients with higher ($P < 0.001$) serum levels of LPA also have larger HCC tumors (>4 cm) and shorter survival compared with those with lower LPA serum concentrations (Fig. 6B,C). To validate our LPA data in HCC patients, publicly ac-

cessible microarray data were analyzed for a correlation between ATX and clinical outcome in HCC patients. ATX expression was significantly increased in HCC patients with more advanced disease, in particular in those with metastatic invasion ($P < 0.001$) (Fig. 6D),[13] and was more strongly expressed in tumoral compared with paired nontumoral tissues (Fig. 6E,F) . In addition, we compared the expression of ATX and LPA receptors in epithelial and stromal components of the same HCC tissues microdissected using the laser capture microscope technique (Fig. 7A,B). We found similar expression levels of ATX in both the epithelial and the stromal component of HCC. However, LPA receptors were essentially expressed in the stromal rather than the epithelial component, indicating the stroma as the main target of the LPA paracrine loop (Fig. 7C). Finally, the ACTA2
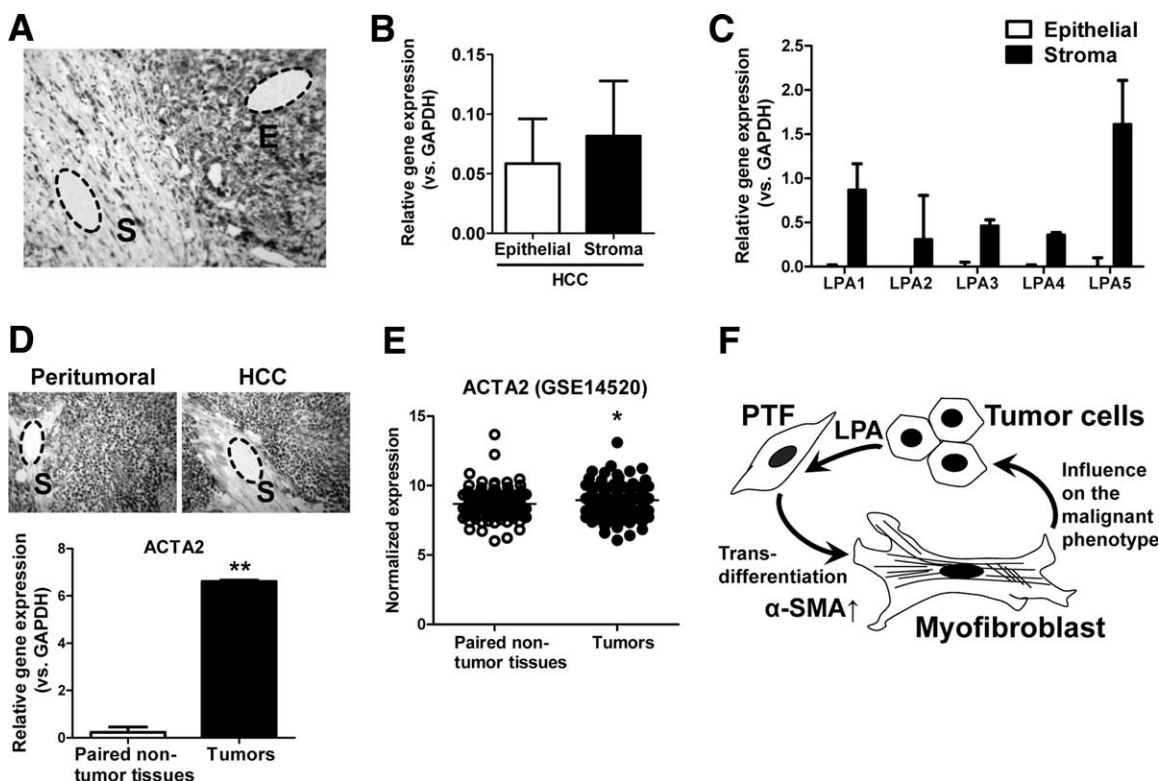
Fig. 7. Evidence for a directional tumor–stroma LPA paracrine loop and for an increased expression of α-SMA as a marker of the myofibroblast phenotype in HCC tissues. (A) Representative image of epithelial and stromal tissues from HCC patients microdissected using the laser capture microscope technique. (B,C) Total RNA was extracted from microdissected tissues, retrotranscribed, and subjected to real-time PCR for (B) ATX and (C) LPA receptor (LPA1-5). Results are expressed as the ratio of the number of ATX or LPA receptors/GAPDH copies and represent the mean ± SEM of three separate experiments, each conducted in triplicate. (D) Representative images of stromal tissues from HCC patients, peritumoral and tumor specimens microdissected using the laser capture microscope technique (top panels). Total RNA was extracted from microdissected tissues, retrotranscribed, and subjected to real-time PCR for ACTA2 (α-SMA) (bottom panel). Results are expressed as the ratio of the number of α-SMA/GAPDH copies and represent the mean ± SEM of three separate experiments, each conducted in triplicate. (E) Publicly available data from the Wang cohort (GSE14520) showing that ACTA2 (α-SMA, a marker for the myofibroblast phenotype) expression levels are increased in HCC (n = 129) compared with paired nontumor tissues (n = 126). *P = 0.0242. (F) A model for the role of LPA in mediating transdifferentiation of PTFs to a CAF-like myofibroblastic phenotype, thus promoting tumor progression of HCC. The illustration shows interactions among cell types in the neoplastic HCC microenvironment, including LPA-driven transdifferentiation of PTFs to a CAF-like myofibroblastic phenotype and, in turn, the influence of this phenotype on malignant cells.

gene was significantly expressed in tumoral compared with paired nontumoral tissues (Fig. 7D). This is consistent with publicly accessible microarray data published by Wang (Fig. 7E). Taken together, these data show that the stromal component represents the main target of LPA in patients with HCC, and that α-SMA–positive cells are predominant within the tumor stroma, as shown by the increased expression of the ACTA2 gene.

Discussion

Although the onset and growth of HCC occurs in tissues with a rich content of local myofibroblasts, the crosstalk between tumor and stroma has been little investigated, despite that fact that in mammary gland development, myofibroblasts display a crucial role in allowing the penetration of end buds into the fat pad during branching morphogenesis or local tumor spread.[14] In this

study, we demonstrate that the interaction between HCC and stroma plays a key role in tumor progression, and that in patients this interaction occurs in more advanced disease. We based our conclusions on the following data: (1) CAFs stimulated proliferation, migration and invasion of HCC cells; (2) HCC cells secreted LPA, which promoted transdifferentiation of PTFs to a CAF-like myofibroblastic phenotype through the up-regulation of genes related to a contractile phenotype; (3) this recruitment and transdifferentiation was blocked by inhibiting LPA secretion; (4) PTFs coinjected with HCC cells accelerated tumor growth and progression, but an LPA inhibitor blocked PTF transdifferentiation and slowed HCC growth and progression; and (5) patients with higher LPA concentrations had larger, metastatic HCC and worse survival.

Myofibroblasts have recently been implicated in HCC progression,[15] but the molecular mechanisms

regulating the interaction between HCC and cells and myofibroblasts are still unknown. We demonstrate for the first time that LPA is involved in the reciprocal cross-talk between HCC cells and resident fibroblasts, leading to tumor progression. In particular, HCC cells activate resident fibroblasts (PTFs), which acquire a contractile capability and express α-SMA, sustained by the up-regulation of specific contractile-related genes giving rise to a myofibroblast-like phenotype. This occurs through a paracrine mechanism, because HCC cells secrete LPA and PTFs express LPA receptors that are absent in HCC cells. LPA is implicated in different malignancies and has recently been shown to induce HCC cell invasion by increasing the production of matrix metalloproteinase-9.[12] Once PTFs have assumed a myofibroblast-like phenotype, in coculture experiments they increase the proliferation, migration, and invasion of HCC cells *in vitro* and promote tumoral progression *in vivo*. We did not investigate mediators of the back cross-talk from myofibroblasts toward HCC cells, but the central role of LPA is further demonstrated by the fact that by blocking LPA with a pharmacological inhibitor or with ATX-silencing, the increased proliferation, migration and invasion of HCC cells is abrogated. *In vivo*, this is even more striking, because after treating animals with an LPA inhibitor, we found a down-regulation of the genes supporting the myofibroblast phenotype and a lower number of activated PTFs, whereas HCC progression decreased. LPA is seen to have a central role in orchestrating the tumor–stroma interaction. This finding is consistent with a previous work showing an alteration of the phospholipid in HCC, where ATX displays a crucial role in the inflammatory peritumoral reaction by interacting with the tumor necrosis factor α/nuclear factor κB pathway.[16] Furthermore, the inhibition of this pathway reduces the protumorigenic activity of CAFs in skin cancer.[17]

In HCC patients, we found increased serum LPA in those with a worse clinical outcome, as also suggested by an analysis of publicly accessible microarray data[13] and by Wang (Personal Communication; http://www.ncbi.nlm.nih.gov/gds?term=gse14520). Our findings are further confirmed by previous work reporting increased levels of LPA in tissues, bile, and serum and in more advanced stages of disease.[13,18] Finally, we also demonstrate that LPA receptors are mainly expressed in stroma rather than epithelium of HCC; consistent with our experimental data, the ACTA2 gene was also more strongly expressed in tumoral tissues than in paired peritumoral tissues. This is supported by analysis of the publicly accessible microarray data from Wang (Personal Communication, http://www.ncbi.nlm.nih.gov/gds?term=gse14520). These data recapitulate those proposed in an *in vivo* model of breast cancer.[19]

In conclusion, our results indicate that LPA plays a central role in orchestrating the cross-talk between HCC cells and resident stromal fibroblasts, and that this promotes HCC progression.

References

1. Colombo M. Natural history and pathogenesis of hepatitis C virus related hepatocellular carcinoma. J Hepatol 1999;31(Suppl. 1):25-30.
2. El Serag HB. Hepatocellular carcinoma: recent trends in the United States. Gastroenterology 2004;127(5 Suppl. 1):S27-S34.
3. Serini G, Gabbiani G. Mechanisms of myofibroblast activity and phenotypic modulation. Exp Cell Res 1999;250:273-283.
4. Tomasek JJ, Gabbiani G, Hinz B, Chaponnier C, Brown RA. Myofibroblasts and mechano-regulation of connective tissue remodelling. Nat Rev Mol Cell Biol 2002;3:349-363.
5. Sappino AP, Skalli O, Jackson B, Schurch W, Gabbiani G. Smooth-muscle differentiation in stromal cells of malignant and non-malignant breast tissues. Int J Cancer 1988;41:707-712.
6. Di TL, Pasquinelli G, Damiani S. Smooth muscle cell differentiation in mammary stromo-epithelial lesions with evidence of a dual origin: stromal myofibroblasts and myoepithelial cells. Histopathology 2003;42:448-456.
7. Orimo A, Gupta PB, Sgroi DC, Arenzana-Seisdedos F, Delaunay T, Naeem R, et al. Stromal fibroblasts present in invasive human breast carcinomas promote tumor growth and angiogenesis through elevated SDF-1/CXCL12 secretion. Cell 2005;121:335-348.
8. Qiu W, Hu M, Sridhar A, Opeskin K, Fox S, Shipitsin M, et al. No evidence of clonal somatic genetic alterations in cancer-associated fibroblasts from human breast and ovarian carcinomas. Nat Genet 2008;40:650-655.
9. Haviv I, Polyak K, Qiu W, Hu M, Campbell I. Origin of carcinoma associated fibroblasts. Cell Cycle 2009;8:589-595.
10. Stracke ML, Krutzsch HC, Unsworth EJ, Arestad A, Cioce V, Schiffmann E, et al. Identification, purification, and partial sequence analysis of autotaxin, a novel motility-stimulating protein. J Biol Chem 1992;267:2524-2529.
11. Mills GB, Moolenaar WH. The emerging role of lysophosphatidic acid in cancer. Nat Rev Cancer 2003;3:582-591.
12. Park SY, Jeong KJ, Panupinthu N, Yu S, Lee J, Han JW, et al. Lysophosphatidic acid augments human hepatocellular carcinoma cell invasion through LPA1 receptor and MMP-9 expression. Oncogene 2011;30:1351-1359.
13. Wurmbach E, Chen YB, Khitrov G, Zhang W, Roayaie S, Schwartz M, et al. Genome-wide molecular profiles of HCV-induced dysplasia and hepatocellular carcinoma. HEPATOLOGY 2007;45:938-947.
14. Williams JM, Daniel CW. Mammary ductal elongation: differentiation of myoepithelium and basal lamina during branching morphogenesis. Dev Biol 1983;97:274-290.
15. van ZF, Mair M, Csiszar A, Schneller D, Zulehner G, Huber H, et al. Hepatic tumor-stroma crosstalk guides epithelial to mesenchymal transition at the tumor edge. Oncogene 2009;28:4022-4033.
16. Wu JM, Xu Y, Skill NJ, Sheng H, Zhao Z, Yu M, et al. Autotaxin expression and its connection with the TNF-alpha-NF-kappaB axis in human hepatocellular carcinoma. Mol Cancer 2010;9:71.
17. Erez N, Truitt M, Olson P, Arron ST, Hanahan D. Cancer-associated fibroblasts are activated in incipient neoplasia to orchestrate tumor-promoting inflammation in an NF-kappaB-dependent manner. Cancer Cell 2010;17:135-147.
18. Skill NJ, Scott RE, Wu J, Maluccio MA. Hepatocellular carcinoma associated lipid metabolism reprogramming. J Surg Res 2011;169:51-56.
19. Liu S, Umezu-Goto M, Murph M, Lu Y, Liu W, Zhang F, et al. Expression of autotaxin and lysophosphatidic acid receptors increases mammary tumorigenesis, invasion, and metastases. Cancer Cell 2009;15:539-550.